IMMUNOLOGY

Increased vaccine tolerability and protection via NF-κB modulation

B. A. Moser[1], R. C. Steinhardt[1], Y. Escalante-Buendia[1], D. A. Boltz[2], K. M. Barker[2], B. J. Cassaidy[1], M.G. Rosenberger[1], S. Yoo[3], B. G. McGonnigal[3], A. P. Esser-Kahn[1]*

Improving adjuvant responses is a promising pathway to develop vaccines against some pathogens (e.g., HIV or dengue). One challenge in adjuvant development is modulating the inflammatory response, which can cause excess side effects, while maintaining immune activation and protection. No approved adjuvants yet have the capability to independently modulate inflammation and protection. Here, we demonstrate a method to limit inflammation while retaining and often increasing the protective responses. To accomplish this goal, we combined a partial selective nuclear factor kappa B (NF-κB) inhibitor with several current adjuvants. The resulting vaccines reduce systemic inflammation and boost protective responses. In an influenza challenge model, we demonstrate that this approach enhances protection. This method was tested across a broad range of adjuvants and antigens. We anticipate these studies will lead to an alternative approach to vaccine formulation design that may prove broadly applicable to a wide range of adjuvants and vaccines.

INTRODUCTION

Vaccines are considered one of the most effective global health interventions against infectious diseases. Current and future vaccines face challenges of more effective and diverse protective responses with ever more stringent safety margins. A major challenge in developing new vaccine approaches and formulations is increasing effective immune activation, leading to protective responses, while limiting the excess inflammation. Determining and maintaining an appropriate balance of providing effective protection while limiting inflammation-induced side effects are cited as critical to successful vaccine design (*1*–*3*). To boost the immune response, Toll-like receptor (TLR) agonists have been explored as vaccine adjuvants because they activate the innate immune system, promoting the expression of a wide variety of immune genes, including inflammatory cytokines and cell surface receptors important for T cell interactions (*4*–*9*). Effective TLR agonists stimulate the desired cellular or humoral adaptive responses and have resulted in several successful vaccines (*10*). However, the inability to directly modulate inflammation has increased vaccine costs and delayed their application (*11*). For example, CpG DNA, a TLR9 agonist, has wide-ranging promise as a vaccine adjuvant and provides protection for diseases currently without a vaccine, such as HIV (*12*, *13*). CpG DNA also enables vaccines to be produced with less antigen (*14*), induces protective responses faster (*15*), and produces effective antitumor activity (*16*, *17*). CpG has demonstrated great promise in increasing seroprotective antibody titers in human clinical trials (*18*, *19*). However, the excessive inflammatory response induced by some vaccine formulations incorporating CpG sequences has increased the cost of its development and reduced the number of vaccines where it has been implemented (*13*, *17*–*19*). Despite the promise of CpG, only one vaccine, HEPLISAV-B created by Dynavax Technologies, has achieved approval for use in humans. Improving the tolerability profile of adjuvants generally, and CpG specifically, might enable its inclusion in additional vaccines (*3*, *20*). CpGs are only a fraction of the hundreds of TLR agonist adjuvants facing similar challenges (*21*). There are now multiple successful TLR agonists available in vaccines, but one challenge with new and high doses of TLR agonists is the excess inflammation resulting from either over activation or systemic distribution (*20*). In rare cases where inflammation leads to reported side effects in vaccine candidates, it is often due to systemic distribution of tumor necrosis factor–α (TNF-α) and interleukin-6 (IL-6) (*22*, *23*). A successful approach to these issues is to alter the structure or formulation of a TLR agonist. However, this approach adds cost and does not alter the underlying activation pathways leading to excess inflammation. Here, we demonstrate a different and generalizable approach to decouple the inflammatory response from the antigen-presenting actions of several adjuvants using a second molecule, an immune potentiator, which can be added to current TLR agonist formulation. Using a broad range of TLR agonists, we demonstrate both in vitro and in vivo that using an immune potentiator decreases proinflammatory cytokines while maintaining and generally enhancing adaptive immune function. In vivo, we find that coadministering the immune potentiator with the 2017–2018 flu vaccine (Fluzone) improves tolerability by decreasing side effects associated with excess inflammation while enhancing protection against influenza. Coadministration of the immune potentiator with CpG-ODN1826 (CpG) and dengue capsid protein leads to elimination of systemic TNF-α and IL-6 after vaccination and yields sustained neutralizing antibodies. Administering the immune potentiator with CpG and gp120, an HIV viral coat protein, increased serum immunoglobulin G (IgG) and vaginal IgA antibodies and shifted IgG antibody epitope recognition. We found additional benefits of immune potentiation, including altered epitope selectivity and subtype distribution for certain antigens. Last, we observed immune potentiation and modulation of inflammation for several TLR agonists—implying a general approach for improving tolerability that might be applied to hundreds of agonists. Immune potentiation

[1]Pritzker School for Molecular Engineering, University of Chicago, 5640 South Ellis Avenue, Chicago, IL 60637, USA. [2]Division of Microbiology and Molecular Biology, IIT Research Institute, Illinois Institute of Technology, 10W. 35th Street, Chicago, IL 60616, USA. [3]Department of Chemistry, Chemical Engineering & Materials Science, Biomedical Engineering, University of California, Irvine, CA 92697, USA.
*Corresponding author. Email: aesserkahn@uchicago.edu

may find use in modulating the inflammation of many adjuvanted vaccines (*24*)—lowering the costs of implementing TLR adjuvants, in some cases, improving their responses, and increasing the diversity of adaptive immune profiles and widening the scope of disease prevention and treatment.

Selection of immune potentiator

In seeking a method of immune potentiation, we explored the extensive research on the TLR activation pathway. This powerful mechanistic framework led us to hypothesize about how TLR activation directs inflammatory cytokines and antigen presentation. As TLR pathways converge with nuclear factor kappa B (NF-κB) activation and inflammatory and adaptive responses diverge upon which NF-κB subunit is activated, we hypothesized that we could decouple these processes via selective inhibition—leading to improved tolerability but maintaining the adaptive response. Upon TLR activation, the transcription factor NF-κB primes the transcription of proinflammatory cytokines such as IL-6 and TNF-α and cell surface receptors such as major histocompatibility complex II (MHCII), CD40, CD80, and CD86 (*25*–*27*). The NF-κB family is a family of transcription factors consisting of two subunits: a DNA binding domain and a transcriptional activator (*28*, *29*). Each NF-κB dimer controls expression of a different set of genes for distinct cellular processes—broadly, some dimers mainly control inflammatory expression, while others control antigen presentation (*28*–*30*). Selectively modulating a pathway, we conjectured, might lead to increased antigen presentation while decreasing inflammation. NF-κB inhibitors have been widely explored for reducing cytokine expression in cancer (*31*–*34*), autoimmune disorders (*35*), and sepsis (*36*–*38*), yet they have not been explored as vaccine potentiators. This lack of experimentation may be because it is broadly understood that NF-κB activation is necessary in mounting an adequate adaptive immune response (*34*, *39*). However, only certain subunits direct antigen presentation, while others lead to inflammation (*40*). As a proof-of-concept immune potentiator, we chose SN50, a cell permeable peptide that consists of the nuclear localization sequence of the NF-κB subunit p50, which blocks the import of p50-containing dimers into the nucleus (*41*, *42*). We consider SN50 to be a partial selective NF-κB inhibitor, where it blocks the import of some NF-κB subunits but not others. However, this inhibitor can also inhibit other transcription factors that use the same importin such as activator protein 1 (AP-1), nuclear factor of activated T cells (NFAT), and signal transducer and activator of transcription 1 (STAT1) (*43*, *44*). NF-κB subunits also have some level of redundancy, where each subunit can prime a wide variety of genes (*45*). However, each NF-κB subunit will have a defined affinity for specific promoters, leading each NF-κB subunit to elicit a different transcriptional response (*46*). For more literature on which genes are primed by each NF-κB subunit, we direct the reader to a variety of studies on this topic (*30*, *46*–*57*). We also expect that SN50 inhibits NF-κB for a relatively short period of time and acts to curb immediate high levels of inflammation from adjuvants in contrast to previous studies where subunit knockouts were used to examine the long-term effects of NF-κB subunits on immunity (*41*, *42*, *47*).

RESULTS

First, we sought to determine whether SN50 enables inhibition of NF-κB in innate immune cells. We validated that SN50 reduced total NF-κB activity in human (THP-1 monocytes) and mouse (RAW macrophages) cells in a dose-dependent manner (fig. S1).

Examination of CpG-induced inflammation and resulting immune response

We sought to verify that SN50 could enable antigen-presenting cells to up-regulate cell surface receptors while limiting proinflammatory cytokine production. We incubated murine bone marrow–derived dendritic cells (BMDCs) with SN50 and CpG or CpG alone for 6 hours and analyzed how the potentiator altered cytokine production and cell surface receptor expression (Fig. 1A). Intracellular cytokine staining revealed that cells treated with SN50 demonstrated a significant decrease in cells expressing TNF-α and IL-6. Meanwhile, CD86 expression increased significantly and CD40 expression was sustained. Because the p65-p50 dimer is the most abundant dimer found in resting cells and involved in inflammatory cytokine production, we conjecture that by inhibiting this dimer, we enable the transcription and translation of cell surface receptors while limiting inflammatory cytokines. This is consistent with previous *p65* knockout experiments that demonstrate the significance of the p65 subunit in increasing inflammatory cytokine production and inhibition of CD40 and CD86 (*40*). The result is lower inflammatory responses while priming effective adaptive immune communication.

After observing that SN50 can limit inflammation without decreasing cell surface receptor expression in vitro, we next wanted to examine the effect in vivo. To determine whether inhibition of NF-κB could decrease the systemic levels of proinflammatory cytokines TNF-α and IL-6 associated with CpG vaccination, we vaccinated mice intramuscularly with 100 μg of ovalbumin (OVA) and phosphate-buffered saline (PBS), SN50 (500 μg), CpG (50 μg), CpG + SN50, or CpG + SN50M (500 μg). SN50M is the commercially available control for SN50 as it is a weaker inhibitor (*42*). We chose to measure systemic levels of proinflammatory cytokines TNF-α and IL-6 because high levels are considered unsafe and lead to side effects (*22*, *23*, *58*). In humans, systemic TNF-α correlates with local side effects (e.g., swelling and pain at injection site), and systemic IL-6 has been correlated with system-wide side effects (e.g., fatigue and headache) in response to vaccination (*22*, *23*). In addition, both of these cytokines act as pyrogens when distributed systemically, leading to a fever response (*58*). We measured these proinflammatory cytokines at 1, 3, 6, 24, and 48 hours after injection in all groups to determine the time point where cytokines peak in response to CpG vaccination (Fig. 1, B and C, and fig. S2). Mice vaccinated with OVA and PBS or SN50 alone elicited no detectable levels of systemic TNF-α or IL-6. CpG demonstrated the highest response of both TNF-α (1325 pg/ml) and IL-6 (1269 pg/ml) at the 1-hour time point. The CpG + SN50 group showed complete elimination of cytokines for both cytokines. The CpG + SN50M group showed a decrease in cytokine levels, although not as large as those observed with CpG + SN50. We hypothesize that this decrease in inflammatory cytokines is due to the high local inhibition of injected SN50M and not physical aggregation, as scanning electron microscopy analysis shows that larger aggregates are not formed with SN50 or SN50M (fig. S2). Examination in vitro shows that there is some inhibition of SN50M, especially at higher concentrations (fig. S1). We also vaccinated mice with an additional peptide control, SM, which has performed as a better control in other studies and performed better in our study (fig. S3) (*42*). To determine how SN50 would affect the humoral response, we analyzed serum antibody levels on day 28

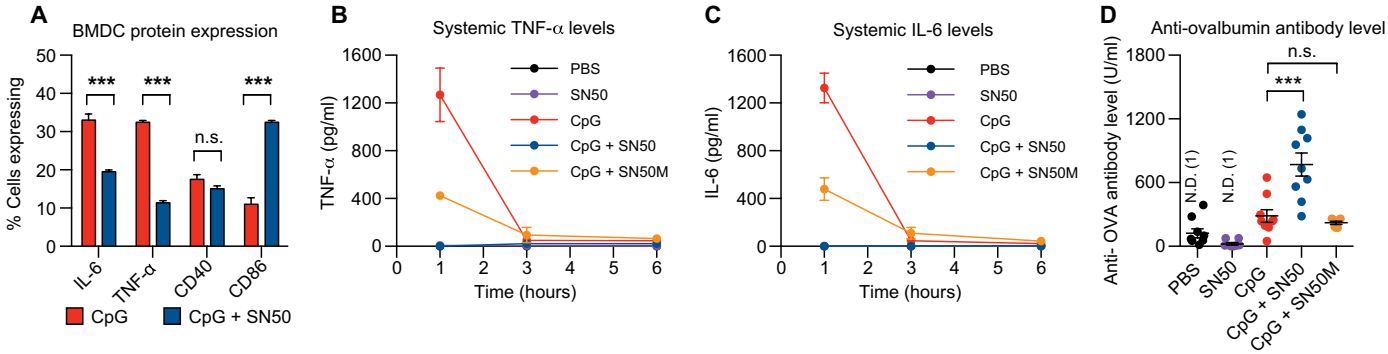

Fig. 1. In vivo vaccination with model antigen OVA and immune adjuvant SN50. (**A**) Intracellular cytokine staining of BMDCs treated with CpG (red bars) or CpG + SN50 (blue bars), $n = 3$. (**B**) Systemic levels of TNF-α measured at 1, 3, and 6 hours after injection with PBS (black line), SN50 alone (purple line), CpG (red line), CpG + SN50 (blue line), and CpG + SN50M (yellow line), $n = 4$ for each time point. (**C**) Systemic levels of IL-6. (**D**) Anti-OVA antibody level, day 28, $n = 8$. $^*P < 0.05$, $^{**}P < 0.01$, and $^{***}P < 0.001$. n.s., not significant.

(Fig. 1D). To broadly establish how the addition of SN50 affects the antibody levels, we chose to use an enzyme-linked immunosorbent assay (ELISA) that measures total Ig (G + A + M) (*59*). The CpG group demonstrated a 2.4-fold increase in anti-OVA antibodies compared with PBS alone. Mice vaccinated with CpG + SN50 demonstrated a 5.9-fold increase over the PBS group and a 2.7-fold increase over the CpG group. These data confirmed our hypothesis that high levels of systemic TNF-α and IL-6 can be decoupled from the humoral, adaptive immune response. We were not expecting to find that addition of SN50 boosted the downstream adaptive response, leading to immune potentiation. Because of this increase in adaptive response and improved tolerability profile after vaccination, we categorize SN50 as an immune potentiator.

This unexpected finding led us to investigate further how SN50 might be potentiating the immune response. First, we analyzed a broader range of cytokines over various time points after vaccination. We vaccinated mice intramuscularly with PBS or 100 μg of OVA and CpG (50 μg) or CpG + SN50 (50 μg of CpG and 500 μg of SN50) and analyzed the plasma at 1, 3, 6, 24, 48, and 72 hours after vaccination for systemic expression of IL-1α, IL-1β, IL-10, IL-12p70, IL-17A, IL-23, IL-27, monocyte chemoattractant protein 1 (MCP-1), interferon-α (IFN-α), IFN-β, IFN-γ, TNF-α, and granulocyte-macrophage colony-stimulating factor (GM-CSF) (Fig. 2A). No systemic IL-1β or IFN-α levels were observed in any group at any time point. TNF-α demonstrated that the CpG induced peak at 1 hour as in our previous experiment, and systemic TNF-α was observed for at least the first 6 hours and CpG + SN50 decreased the level of TNF-α to background levels. In contrast to a complete lowering of cytokines, SN50 altered the timing of some cytokines. MCP-1 levels in CpG + SN50 at early time points were lower compared with CpG at 3, 6, and 24 hours, but at 24 hours, levels started to rise and CpG-alone levels began to fall. In further contrast, SN50 boosted some cytokine levels. Systemic IL-23 levels were higher at 1 hour after vaccination in CpG + SN50 than in CpG alone. These data demonstrate that SN50 does not dampen the immune response but alters the cytokine profile.

Given the alteration in temporal and systemic immune responses, we wanted to examine changes to the draining lymph node 24 hours after vaccination. Because we were unsure of what changes might occur, we used gene expression data rather than focusing on a single cytokine. We vaccinated mice intramuscularly with OVA only, OVA and CpG (CpG), or OVA and CpG + SN50 (CpG + SN50) and analyzed gene expression in the draining inguinal lymph node 24 hours after vaccination (Table 1 and figs. S4 and S5). We found that for CpG + SN50 mice, *cd86* expression was slightly increased compared with CpG alone, indicating that SN50 does not dampen expression of this important cell surface receptor but rather increases it—matching our in vitro experiments. In addition, in CpG + SN50 mice, *cxcl10* and *cxcl11* were both increased compared with CpG group by 3.4- and 10-fold, respectively. These genes are important chemoattractants for T cells, which could indicate enhanced T cell infiltration into the lymph node. Some genes were decreased in the CpG + SN50 group, such as *cxcr3*, where expression was decreased by threefold compared with the CpG group. The CpG + SN50 had a 10-fold increase in *edn1* expression compared with CpG alone. *Edn1* is expressed by mature dendritic cells, improves the ability to activate T cells, and increases DC survival time (*41*). The CpG + SN50 group demonstrated slightly increased *gzmb* expression compared with the CpG group, further supporting the hypothesis that SN50 does not hamper the ability of APCs to activate T cells. The addition of SN50 also increased the local expression of *ifny*. In addition, although gene expression of *il6* was slightly higher in the lymph nodes from mice without SN50 (twofold higher), we still observed a large increase in gene expression of *il6* compared with OVA alone (147-fold). *Tnfa* expression in the lymph node was actually increased slightly compared with CpG alone (1.4-fold). Together, these results show that high levels of systemic cytokine expression is not required for adequate local expression and that limiting the systemic cytokine levels through the use of SN50 does not diminish local expression in the lymph node. Thereby, adaptive immune signaling is still able to occur. The addition of SN50 increased *nos2* expression by 18-fold. Some adjuvants such as complete Freund's adjuvant have been shown to enhance the immune response through robust *nos2* expression (*60*). These data demonstrate that SN50 alters the local immune response in a variety of ways and that key genes required for T cell chemotaxis, germinal center formation, and innate-adaptive immune communication are maintained or even increased. On the basis of these data, we hypothesized that T cell responses in mice vaccinated with SN50 would be enhanced. To test this, we vaccinated mice as described above with CpG, CpG + SN50, OVA, or PBS, administered a boost on day 14, and analyzed antigen-specific T cell responses on day 21 (Fig. 2B and fig. S6). We found that OVA-specific T cell responses were generally

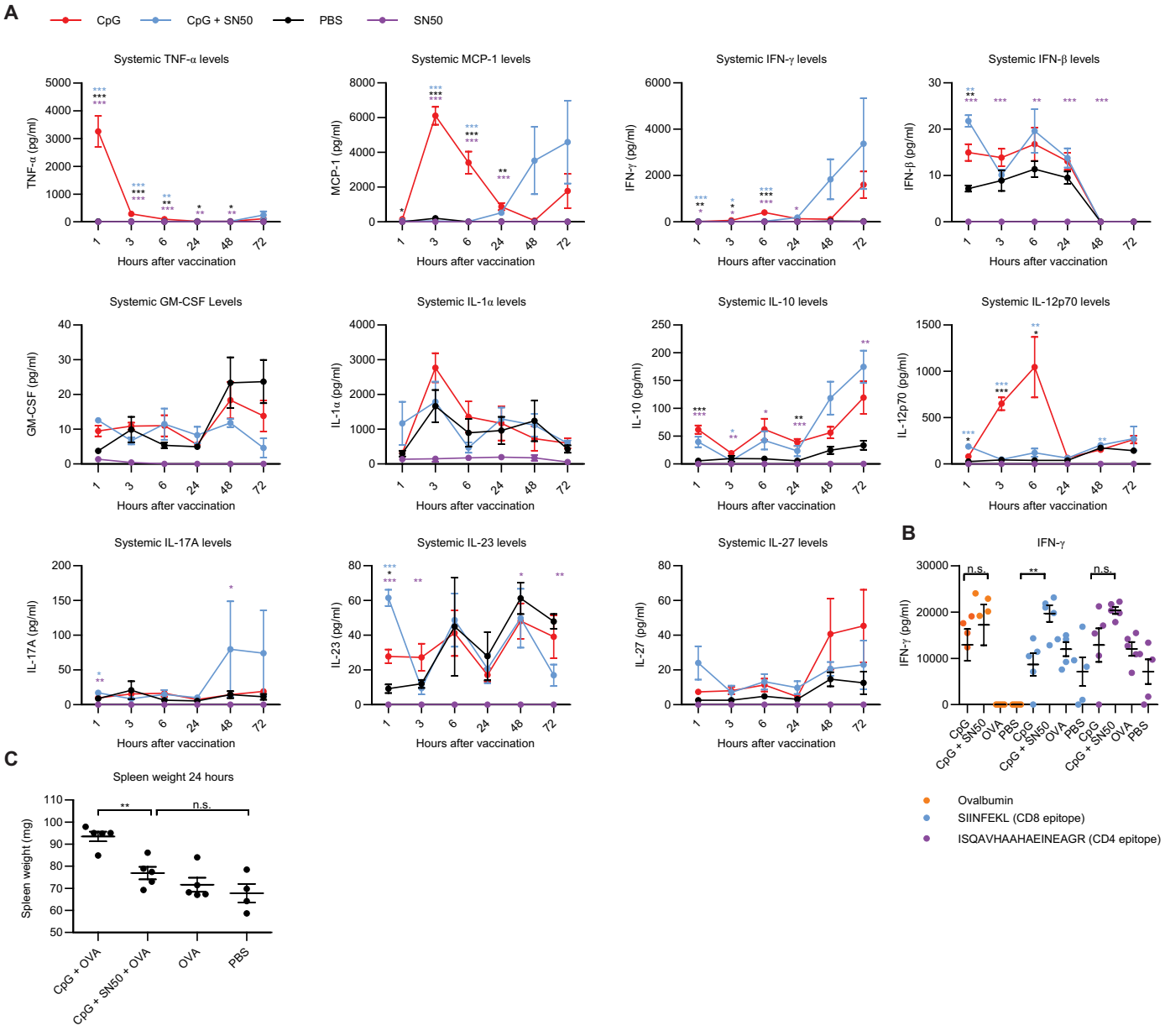

Fig. 2. Examination of broader immune response induced by SN50. (**A**) Systemic levels of cytokines 1, 3, 6, 24, 48, and 72 hours after vaccination with OVA and CpG (red), CpG + SN50 (blue), PBS (black), or SN50 (purple). $n = 5$, significance compared with CpG. (**B**) Splenocytes on day 21 after initial vaccination stimulated with full OVA protein (orange), SIINFEKL (blue), or ISQAVHAEINEAGR (purple). $n = 5$. (**C**) Spleen weight 24 hours after vaccination. $n = 5$. $^*P < 0.05$, $^{**}P < 0.01$, and $^{***}P < 0.001$. n.s., not significant.

increased, with cells stimulated with the CD8 epitope SIINFEKL showing the largest differences (Fig. 2B). In addition to IFN-γ, we also saw significant differences in secretion of IL-5, IL-17A, IL-22, IL-23, and TNF-α (fig. S6). Because CpG is known to induce splenomegaly (*61*), we also examined what affects SN50 would have on this side effect. We vaccinated mice as described above and analyzed the spleen weight 24 hours after vaccination and on day 21 (Fig. 2C and fig. S7). We found that CpG induced splenomegaly, with spleen weights 1.3-fold larger than the OVA alone. The addition of SN50 completely reduced the level of splenomegaly to background levels. Without SN50, splenomegaly continued to increase to 2.3-fold higher than OVA-only levels through day 21. This directly demonstrates that SN50 can reduce a challenging side effect from CpG-induced vaccination.

To further understand how SN50 acts to potentiate the immune response, we examined the effect of location and systemic injection of SN50. We found that SN50 must be present at the site of injection and does not work by systemic distribution (fig. S8). To understand how decreasing the inflammatory cytokines TNF-α and IL-6 affects the innate and adaptive immune responses, we also examined the effect of coinjection of TNF-α–neutralizing antibody or IL-6–neutralizing antibodies (fig. S8). Although both of these antibodies decreased systemic levels of TNF-α or IL-6, there was no effect on the production of anti-OVA antibodies. This result demonstrates

Table 1. Gene expression in the draining lymph node. Twenty-four hours after vaccination with OVA and CpG or CpG + SN50, fold change relative to vaccination with OVA only. $n = 3$.

Gene	CpG	*P* value	CpG + SN50	*P* value
Gapdh	1.0		1.0	
Cd40	8.1	0.436	6.5	0.015
Cd86	4.5	0.154	7.6	0.004
Cxcl10	25.7	0.027	88.8	0.020
Cxcl11	45.5	<0.001	425.7	0.005
Cxcr3	4.0	0.042	0.9	0.173
Edn1	3.3	0.005	33.3	0.013
Gzmb	109.1	0.217	157.9	0.038
Ifng	9.6	0.012	55.2	0.028
Il6	278.1	0.425	146.6	0.003
Nos2	6.9	0.104	126.9	0.208
Tnf	2.5	0.615	3.5	0.196

that simply limiting inflammation is not sufficient for the potentiation demonstrated through the addition of SN50.

Immune potentiation in in vivo influenza challenge model

We next wanted to focus on how SN50 might transition to a vaccine with a viral challenge. We selected influenza vaccine as a proof-of-concept vaccination both due to its universality and the relative ease of running animal challenges with multiple parameters. We sought to determine whether SN50 would reduce side effects associated with strong adjuvanticity and to see what effect this alteration on systemic cytokines would have on protection. We vaccinated mice intramuscularly with Fluzone Quadrivalent vaccine (Fz) for the 2017/2018 influenza season, with or without CpG (50 μg) as an immune adjuvant and 500 μg of SN50 (SN50 H) or 50 μg of SN50 (SN50 L) as an immune potentiator. The Fz + SN50 group demonstrated lower levels of TNF-α than Fz alone (Fig. 3, B and C). Across all groups, the addition of SN50 reduced levels of TNF-α and IL-6 to levels consistent with the placebo group. To examine whether SN50 can mitigate side effects from vaccination, we analyzed the percent change in body weight 24, 48, and 72 hours after vaccination (Fig. 3D and fig. S9). Weight loss is the easiest and most objective measure of side effects in mice. Mice vaccinated with Fz and Fz + SN50 lost an average of 0.85 and 0.75%, respectively, by the 24-hour time point. The Fz + CpG group lost an average of 5.9%. Adding SN50 H decreased the amount of weight loss to 2.4%, and adding SN50 L to 5.1%. At 72 hours, the Fz group were −1.1% of the starting weight, whereas mice vaccinated with Fz + SN50 gained +1.5%. The Fz + CpG group lost −1.6% of the starting weight, and adding SN50 H led to a reduction in weight loss (0% change) and adding SN50 L led to −1.3% change. Overall, mice with SN50 lost less weight than mice without SN50, demonstrating that SN50 lowered the side effects associated with vaccination and improved the tolerability of the vaccine.

On day 28, we analyzed the serum for antibody levels in the blood (Fig. 3E and figs. S10 and S11). There was no significant difference in serum IgG concentration between Fz and Fz + SN50. There was a significant difference between Fz samples and Fz + CpG of 2.9-fold. There was no significant difference between groups vaccinated with CpG, implying that the addition of SN50 reduces inflammation and side effects from vaccination, improving tolerability, while maintaining the antibody concentration. We also did not observe significant changes in the IgG1:IgG2c ratios at any time point with the addition of SN50, indicating that the adjuvant, and not SN50, directs the helper T (Th) bias.

We next sought to determine whether including SN50 in the vaccination would increase the protection of Fluzone. At this stage, no additional SN50 was administered to the mice, so only the adaptive immune response induced by the vaccine and subsequent boost would act to protect the mice from influenza. Mice were lethally challenged intranasally with 10^5 plaque-forming units (PFU) A/Michigan/45/2015. On day 3 after challenge, we analyzed the lungs of three mice for viral titer (fig. S12). Survival was analyzed for 14 days after challenge (Fig. 3F). By day 7, all placebo mice and 60% of the Fz mice had reached the humane end point and were euthanized. All other mice survived. The Fz + SN50 group was significantly more protected than the Fz alone group. The addition of SN50 to Fz + CpG confers equal protection, while improving side effects and tolerability from the initial vaccination. Adding SN50 to Fz conferred enhanced protection equal to the Fz + CpG group. This demonstrates that SN50, in addition to improving tolerability, can also enhance the adaptive immune potential of the vaccine. We plan to examine how SN50 achieves this result in subsequent investigations, but the evidence with the OVA model suggests that cellular responses are enhanced with the addition of SN50.

Mice were analyzed for change in body weight and body temperature for 14 days after challenge (Fig. 3, G and H, and fig. S12). The peak average weight loss between Fz (−9.9%) and Fz + SN50 (−2.67%) was statistically significant. Greater weight loss is associated with a more intense infection. These data demonstrate that adding SN50 to Fz improves the response to infection. Addition of SN50 to Fz + CpG demonstrates no significant change in weight loss, indicating that the SN50 can reduce systemic TNF-α and IL-6 and side effects from vaccination with no detrimental effects to the protective response. In the case of influenza, Fz + CpG produces a high-quality immune response that confers adequate protection. Therefore, establishing whether SN50 enhances the protective response or simply maintains the response is challenging. However, because of the decrease in side effects and increase in tolerability profile after vaccination, the addition of SN50 enhances the quality of the vaccine. In addition, highly enhanced vaccine protection was observed when SN50 was combined with Fz alone, indicating that in certain cases, the immune potentiator may serve to boost vaccine protection without a need to incorporate additional adjuvants.

As an additional parameter of disease pathology, we examined body temperature after challenge. Unlike in humans, mice demonstrate a reduction in body temperature upon infection (*62*). The placebo has the largest peak drop in temperature (−4.57°C), followed by the Fz group (−1.58°C) (Fig. 3H). Adding SN50 to Fz or Fz + CpG mitigated the decrease in temperature across all groups.

Tolerability and protection of new vaccine adjuvants are typically considered two interdependent variables with an inverse relationship, where adequate protection is acquired by limiting tolerability or vice versa. As this potentiator makes the vaccine both safer and more protective, we sought a single way to analyze how SN50 was changing the tolerability and protection profile. As these variables are considered inversely related, there are few precedents for correlation. However, a common scoring system used widely across

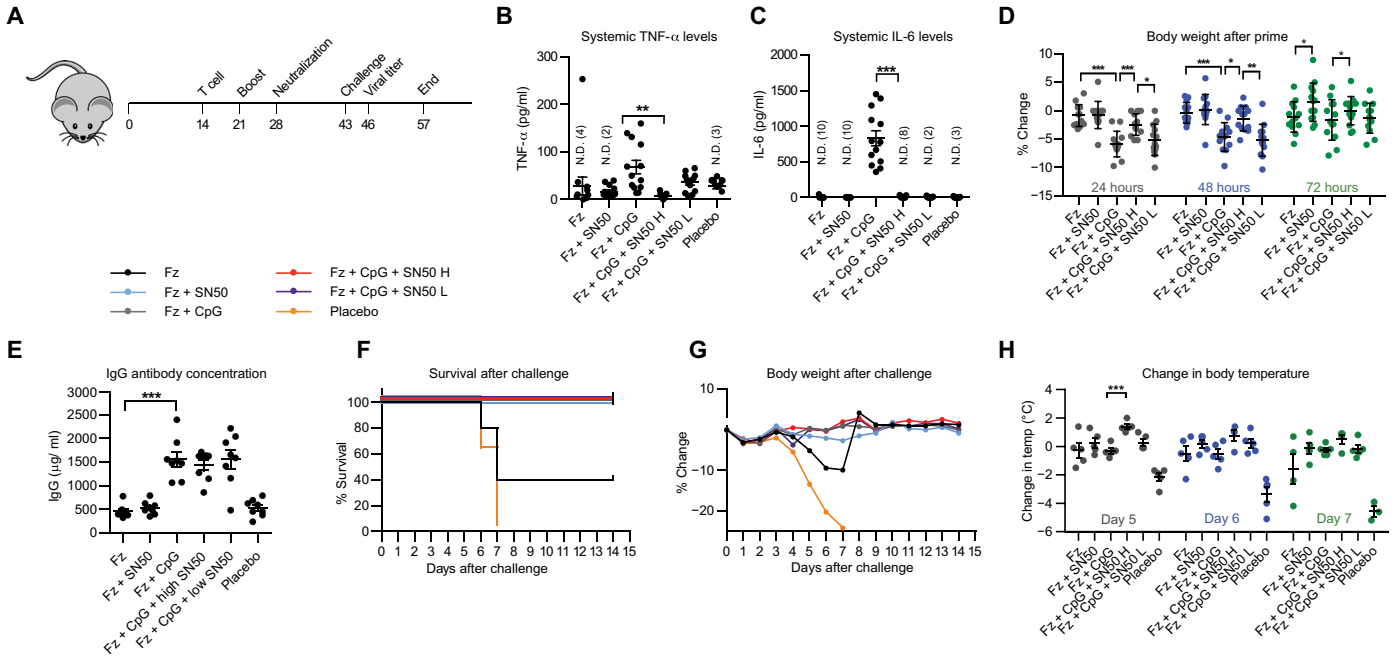

Fig. 3. Influenza challenge model. (**A**) Schematic of influenza challenge study. (**B**) Systemic TNF-α levels 1 hour after vaccination with Fz, Fz + SN50, Fz + CpG, Fz + CpG + SN50 H, Fz + CpG + SN50 L, and placebo. $n = 13$. (**C**) Systemic IL-6 levels 1 hour after vaccination, $n = 13$. (**D**) Percent change in body weight at 24 (gray), 48 (blue), and 72 hours (green) after vaccination, $n = 13$. (**E**) Day 28 IgG antibody concentration, $n = 8$. (**F**) Survival 1 to 14 days after challenge, $n = 5$. Legend above. Groups: Fz (black), Fz + SN50 (blue), Fz + CpG (gray), Fz + CpG + SN50 H (red), Fz + CpG + SN50 L (purple), and placebo (orange), $n = 5$. (**G**) Percent change in body weight at 1 to 14 days, $n = 5$. (**H**) Body temperature at 5 to 7 days after challenge, $n = 5$. $^*P < 0.05$, $^{**}P < 0.01$, and $^{***}P < 0.001$. N.D., not detected.

fields is a quartile-based scoring system (*63*–*66*). Following precedent for scoring systems, we developed a tolerability-versus-protection plot (fig. S13). This plot is meant only to serve as a visual representation of all data collected within this study. All groups that included SN50 in the vaccination increased both the tolerability profile and the protection of the vaccine. When all data are taken together, we conclude that SN50 acts as an immune potentiator by both increasing the tolerability profile and improving the protective outcome of the vaccination.

Next, we wanted to examine whether this type of immune potentiator could improve tolerability and maintain the adaptive response across a broader range of diseases and antigens. We chose to model vaccines against dengue and HIV because they represent additional, important diseases with active vaccine research. In each case, challenges with current methods have been identified, and we wanted to see whether SN50 could help address those challenges as well as maintain the current function of vaccination strategies. For dengue, the main challenge is producing antibodies that neutralize the virus, inhibiting cellular uptake. For HIV, a key challenge is generating IgA antibodies at the mucosal interface as well as eliciting broadly neutralizing antibodies targeted to select epitopes. To explore how adding an immune potentiator affects each of these responses, we analyzed each antigen set in greater detail.

Examination of immune potentiator on dengue neutralization

To explore dengue, we vaccinated mice with the capsid protein of dengue serotype 2 (DENV-2C) and CpG (50 μg), CpG + 500 μg SN50. As for other antigens with CpG, SN50 completely eliminated expression of systemic TNF-α and IL-6 (Fig. 4, A and B). On day 28, we analyzed the difference in antibody concentration (Fig. 4C). Antibody concentration in CpG + SN50 mice was almost twofold higher than the CpG group.

To determine whether SN50 alters the neutralization potential, we analyzed the neutralizing titer for four strains of dengue (Fig. 4D). We tested four serum samples against one strain representative of each dengue serotype. The differences in neutralization potential were not significantly different between the two groups, implying that, similar to our flu results, SN50 improved the tolerability profile while maintaining the protective responses of vaccination.

Analysis of influence of immune potentiator on HIV vaccination

To further test the efficacy of vaccines with SN50 and to attain a broader picture of the induced humoral immune response, we vaccinated mice with gp120, a viral coat protein from HIV necessary for infection and a target of many HIV vaccines, using CpG as the immune adjuvant. Mice vaccinated with CpG demonstrated high levels of both TNF-α and IL-6, whereas all other groups including mice vaccinated with CpG + SN50 demonstrated nondetectable levels of these systemic cytokines at the 1-hour time point (Fig. 4, E and F). On day 28, we analyzed the serum anti-gp120 antibody concentration. The CpG + SN50 group induced a 4.7-fold higher anti-gp120 IgG antibody level than the CpG group in the serum (Fig. 4, G and H). This demonstrates that the addition of SN50 increases IgG antibody levels across multiple antigens and suggests that it may serve as a general immune potentiator. Because mucous membranes are particularly susceptible to HIV infection, we also measured the anti-gp120 IgG and IgA antibody concentration in vaginal secretions (Fig. 4, I and J). The CpG + SN50 group demonstrated a 4.4-fold

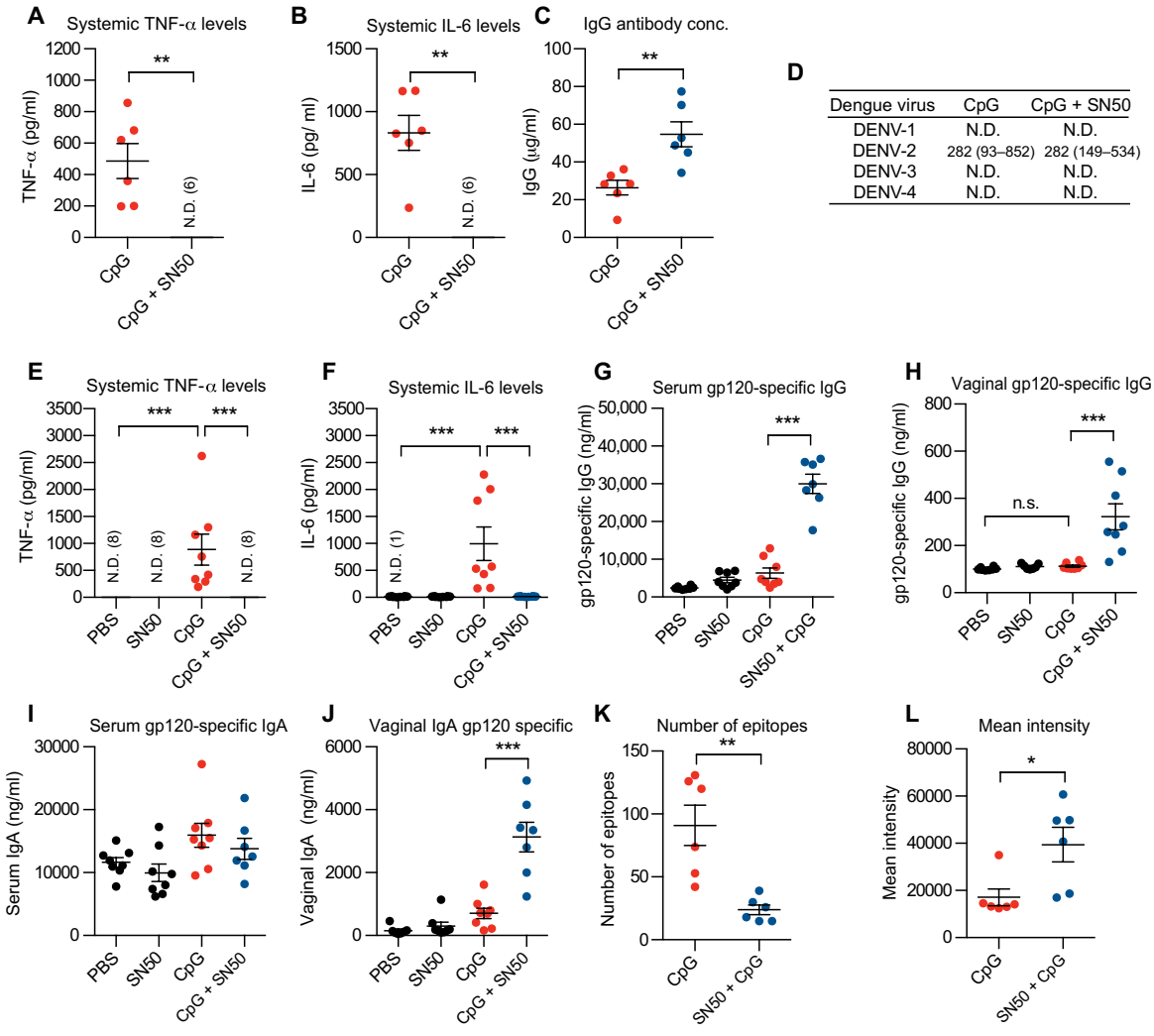

Fig. 4. In vivo vaccination against dengue and HIV. (**A**) Systemic TNF-α levels 1 hour after vaccination with DENV-2C antigen and CpG or CpG + SN50, $n = 6$. (**B**) Systemic IL-6 levels 1 hour after vaccination with DENV-2C antigen and CpG or CpG + SN50. (**C**) IgG antibody concentration on day 28 after vaccination with DENV-2C antigen. (**D**) Dengue virus neutralization. Geometric mean (95% confidence interval). (**E**) Systemic TNF-α levels measured at 1 hour after injection with gp120 and PBS, CpG, SN50, and SN50 + CpG, $n = 8$. (**F**) Systemic IL-6 levels measured at 1 hour after injection with gp120 vaccinations. (**G**) Serum anti-gp120 IgG antibody concentration, day 28 after vaccination with gp120. (**H**) Vaginal anti-gp120 IgG antibody concentration, day 28. (**I**) Serum anti-gp120 IgA antibody concentration, day 28. (**J**) Vaginal anti-gp120 IgA antibody concentration, day 28. (**K**) Number of g120 epitopes recognized by mice vaccinated with CpG or SN50 + CpG. (**L**) Mean intensity of recognized epitopes. $^{*}P < 0.05$, $^{**}P < 0.01$, and $^{***}P < 0.001$.

increase in anti-gp120 IgA antibodies than mice vaccinated with CpG alone. These results suggest that SN50 with gp120 may help induce class-switching to IgA antibody isotype.

The increased values and alteration in IgA levels made us curious about how gp120 was being processed, so we next examined alterations in the gp120 epitopes recognized by the resulting antibodies, using an overlapping peptide microarray (fig. S14). The number of epitopes recognized by CpG alone was higher than antibodies collected from CpG + SN50 mice; however, the fluorescence mean intensity of recognized epitopes is higher in the CpG + SN50 mice (Fig. 4, K and L)—implying a higher concentration of antibodies against those epitopes. From these data, we demonstrate that the addition of SN50 shifts the epitope selectivity in the case of gp120. This may prove valuable with diseases where the current recognized epitopes are not effective at providing protection.

Improvement of adjuvant responses across a variety of TLRs and species

To examine the effects of the SN50 across a broad range of TLR agonists, we performed quantitative polymerase chain reaction (qPCR) on RAW macrophages treated with SN50 followed by stimulation with agonists of different TLRs. We stimulated cells with SN50 and lipopolysaccharide (LPS; 10 ng/ml), CpG (5 μg/ml), R848 (1 μg/ml), and Pam3CSK4 (100 ng/ml) and compared transcript levels to cells treated with TLR agonist alone (Fig. 5A). We chose these TLR agonists because they represent a subset of the compounds with promising potential for commercial use if the inflammatory side effects could be controlled. In RAW macrophages, we observed down-regulation of *TNF*-α and *IL-6* proinflammatory cytokine transcript levels. Across all agonists, the cell surface receptors CD86 and MHCII transcript levels were up-regulated, compared

with agonist alone. This matches with our in vivo observation of increases in *cd86* expression within the lymph node and increased cellular activity when using SN50 with CpG and suggests that the same effects of increased T cell response and increased expression of genes associated with cell migration and cytotoxicity in T cells would be maintained for most adjuvants.

To examine how this would translate in vivo, we vaccinated mice with CpG (50 μg), Pam3CSK4 (20 μg), and R848 (50 μg) using gp120 as the antigen. We chose to run these adjuvants alongside the most widely used adjuvant, alum (250 μg).

With CpG, we observed complete elimination of systemic TNF-α and IL-6 proinflammatory cytokines (Fig. 5, B and C). With R848 and Pam3CSK4, we saw a significant decrease in both TNF-α and IL-6. We hypothesize that SN50 is less effective at decreasing cytokines with R848 because of the low molecular weight of the R848 molecule, enabling more rapid systemic distribution. Alum alone did not evoke a systemic cytokine response, and the addition of SN50 did not alter the cytokine profile. The addition of SN50 increased the average antibody levels for all adjuvants, including alum; however, it was not a statistically significant increase for Pam_3CSK_4 and R848. These data demonstrate that SN50 can be used to decrease systemic inflammation over a wide range of adjuvants while maintaining or even increasing the adaptive response. This demonstrates the broad potential use of this system to a large number of immune adjuvants (Fig. 5D).

To understand how this effect may translate to human vaccinations, we treated THP-1 monocytes with LPS (1 μg/ml) with or without SN50. Cells treated with SN50 and LPS expressed markedly lower levels of TNF-α and IL-6 (Fig. 5E). We also observed increased levels of CD40 and CD86 (Fig. 5F). In addition, we examined the effects of SN50 on primary peripheral blood mononuclear cells (PBMCs) from nonhuman primate (NHP) rhesus macaque. We stimulated NHP PBMCs with SN50 and LPS or LPS alone for 6 hours and analyzed the cell supernatant for proinflammatory cytokines. Cells stimulated with LPS demonstrated high levels of TNF-α and IL-6 in the cell supernatant, and cells with SN50 demonstrated significant reduction in cytokine levels (Fig. 5G). We observed that CD86 expression was increased by twofold in cells stimulated with SN50 and LPS compared with cells stimulated with LPS alone (Fig. 5H). This implies that SN50 may work similarly in NHP and humans as it does in mice.

DISCUSSION

Using a broad range of TLR agonists, we show both in vitro and in vivo that a cell permeable inhibitor of the p50 subunit of NF-κB potentiates the immune response—reducing inflammation and side effects while increasing antibody responses. Coadministration of CpG with the immune potentiator results in significantly reduced levels of systemic proinflammatory cytokines, often to undetectable

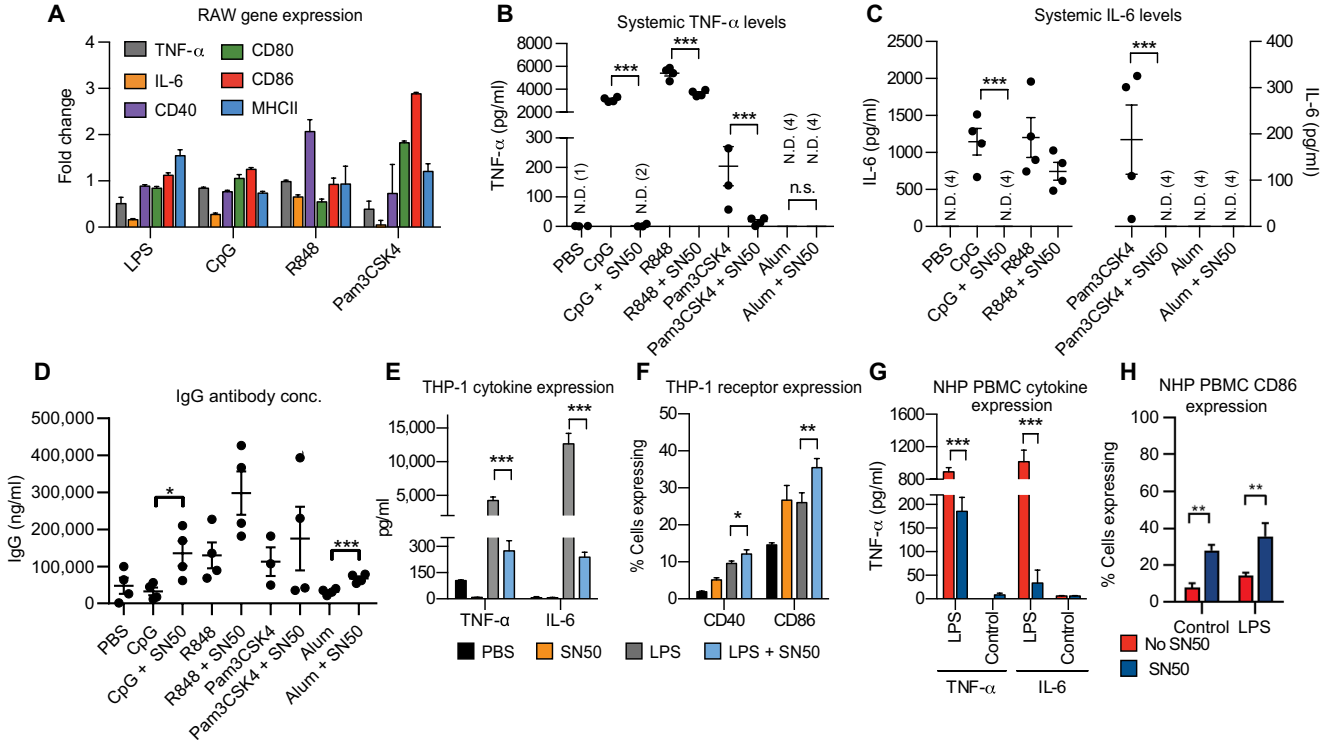

Fig. 5. In vivo vaccinations across a broad range of adjuvants. (**A**) qPCR gene expression analysis of RAW macrophages stimulated with SN50 and TLR agonists compared with cells stimulated with TLR agonist alone. Proinflammatory cytokines TNF-α (gray bars) and IL-6 (orange bars) and cell surface receptors CD40 (purple bars), CD80 (green bars), CD86 (red bars), and MHCII (blue bars). (**B**) Systemic TNF-α cytokine levels of TNF-α measured at 1 hour after injection with gp120 and PBS, CpG, CpG + SN50, Pam3CSK4, Pam3CSK4 + SN50, R848, R848 + SN50, alum, and alum + SN50, $n = 4$. (**C**) Systemic IL-6 cytokine levels measured at 1 hour after injection. (**D**) Serum IgG antibody concentrations, day 28. (**E**) Human THP-1 cell proinflammatory cytokines TNF-α and IL-6 in cell supernatant after treatment with PBS (black bars), SN50 (orange bars), LPS (gray bars), or LPS + SN50 (blue bars). (**F**) Cell surface receptor expression on human THP-1 cell after treatment with PBS (black bars), SN50 (orange bars), LPS (gray bars), or LPS + SN50 (blue bars). (**G**) Cytokine expression analysis of TNF-α and IL-6 in cell supernatant of NHP PBMCs 6 hours. No SN50 (red bars), SN50 (blue bars). LPS (1 μg/ml). (**H**) CD86 expression of NHP PBMCs 18 hours. No SN50 (red bars), SN50 (blue bars). *$P < 0.05$, **$P < 0.01$, and ***$P < 0.001$.

levels. At the same time, the addition of the immune potentiator results in a threefold increase in the IgG levels of antibodies for the model antigen OVA. This indicates that it is possible to potentiate the adaptive immune response while limiting inflammation from the innate immune system. We examined how potentiation would enhance the capabilities of adjuvant to improve the immune response. In our influenza model, we directly examined side effects in response to the current commercial flu vaccine and Fz + CpG and determine that adding SN50 reduces side effects and systemic proinflammatory cytokine levels, improving the tolerability of the vaccine. We also demonstrate that the tolerability profile can be enhanced without negatively effecting—and in most cases—improving the protective response. After vaccinated mice were challenged with influenza A, mice with SN50 added to the vaccine had increased survival, less weight loss, and less change in body temperature, demonstrating that SN50 enhances protection. To study the effects of potentiation on TLR agonists as vaccine adjuvants, we selected three diseases—influenza, dengue, and HIV—all of which have had different challenges in vaccine development. In dengue vaccination, the goal is to increase antibody neutralization potential while maintaining a safe profile. We demonstrate that there are no detrimental effects to dengue neutralization of antibodies with the addition of SN50, enabling us to mitigate side effects but maintain the protective response. In HIV, we vaccinated with HIV envelope protein gp120, CpG, and SN50, which increased both IgG and IgA levels. Analysis of antibodies produced through vaccination with SN50 demonstrates a shift in recognized epitopes. This could be useful in creating antibodies against epitopes that have previously been difficult to achieve using conventional methods. While very preliminary, the increased IgA levels warrant further investigation as few adjuvants have demonstrated a capability to increase IgA levels. The alteration of NF-κB signaling appears quite general as it potentiates the adaptive response with many TLR agonists and antigens. In addition, we demonstrate that directly inhibiting the local inflammatory response at the injection site does not negatively affect the adaptive response. SN50 is one of hundreds of similar NF-κB potentiators (*67*). When used in combination with the appropriate TLR agonist, many potentiators may prove useful for eliciting specific and potentially tunable responses for distinct vaccines or immunotherapies. This methodology may find use in reducing the systemic side effects associated with inflammation seen in many vaccines that elicit inflammation via NF-κB signaling (*24*). This method has the potential to enable a wider range of pattern recognition receptor (PRR) agonists to be used safely in vaccines and to expand the window under which adjuvants can be safely administered. It may also increase the diversity of adaptive immune profiles and widen the scope of disease prevention and treatment.

In conclusion, we have demonstrated that using a specific NF-κB inhibitor in combination with common immune adjuvants can decrease systemic proinflammatory cytokine production while boosting cell surface receptor expression for effective antigen presentation and T cell activation in mouse, human, and NHP primary cells. The use of this inhibitor in vivo completely reduced systemic TNF-α and IL-6 to baseline levels while increasing the downstream adaptive humoral response from the vaccination. These phenomena were observed across a broad range of antigens for a variety of pathogens, demonstrating that this may prove a general strategy for improving vaccination response while conforming to strict safety standards. There are hundreds of documented immune adjuvants that provide adequate protection against diseases, but the inability to independently modulate inflammation and side effects limit their use. (*11*, *68*) In addition, there are hundreds of NF-κB inhibitors, some already with U.S. Food and Drug Administration approval, which could be multiplexed with different TLR agonists to provide a broad range of immune responses (*42*). We anticipate this framework will enable a variety of TLR agonists to be used safely in human vaccines, increasing the diversity of adaptive immune profiles and widening the scope of disease prevention and treatment.

MATERIALS AND METHODS

Study design

The overall objective of this study was to investigate the effect of SN50 on early innate immune responses and adaptive immune responses. Randomization was performed in the influenza challenge study. Otherwise, no randomization or blinding was performed. The experiments were designed to maximize data collection using fewer animals and to be able to include controls such as PBS injection and SN50 alone for comparison. The sample sizes were chosen on the basis of preliminary experiments or literature precedent. Number of animals analyzed is stated in the figure legends.

RAW-Blue NF-κB assay

RAW-Blue NF-κB cells (InvivoGen) were passaged and plated in a 96-well plate at 100,000 cells per well in 180 μl of Dulbecco's modified Eagle's medium (DMEM) containing 10% heat-inactivated fetal bovine serum (HIFBS). Cells were incubated at 37°C and 5% CO_2 for 1 hour. SN50 was added at indicated concentrations; cells were incubated for 1 hour. Immune agonists were added at their indicated concentrations. The volume of each well was brought to 200 μl and incubated at 37°C and 5% CO_2 for 18 hours. After 18 hours, 20 μl of the cell supernatant was placed in 180 μl of freshly prepared QuantiBlue (InvivoGen) solution and incubated at 37°C and 5% CO_2 for up to 2 hours. The plate was analyzed every hour using a Multiskan FC plate reader (Thermo Fisher Scientific), and absorbance was measured at 620 nm.

THP-1 blue NF-κB assay

THP-Blue NF-κB cells (InvivoGen) were passaged and plated in a 96-well plate at 400,000 cells per well in 180 μl of RPMI 1680 containing 10% HIFBS. Cells were incubated at 37°C and 5% CO_2 for 1 hour. SN50 was added at indicated concentrations, and cells were incubated for 1 hour. Immune agonists were added at their indicated concentrations. The volume of each well was brought to 200 μl and incubated at 37°C and 5% CO_2 for 18 hours. After 18 hours, the plate was spun down at 400*g* (Allegra X-30, Beckman Coulter), and 20 μl of the cell supernatant was placed in 180 μl of freshly prepared QuantiBlue (InvivoGen) solution and incubated at 37°C and 5% CO_2 for up to 2 hours. The plate was analyzed every hour using a Multiskan FC plate reader (Thermo Fisher Scientific), and absorbance was measured at 620 nm.

Gene expression

RAW 264.7 macrophages or THP-1 cells were passaged and plated in a cell culture–treated six-well plate at 4×10^6 cells per well in 1.5 ml of DMEM or RPMI (respectively) containing 10% HIFBS. SN50 (250 μg/ml) or PBS was added to wells, and cells were incubated

for 1 hour at 37°C and 5% CO_2 for 6 hours. RNA was extracted using RNeasy Plus Mini Kit (Qiagen). Reverse transcription PCR was performed using RT2 First Strand Kit (Qiagen) and Bio-Rad thermocycler according to the manufacturer's protocol. Complementary DNA (cDNA) was stored at −20°C. RT2 SYBR ROX qPCR Master Mix (Qiagen) was used according to the manufacturer's protocol. qPCR amplification was performed using a Stratagene Mx3005P thermocycler.

Flow cytometry

All antibodies were purchased from BioLegend or Thermo Fisher Scientific. Antibodies used in this study include the following: mouse—allophycocyanin (APC) TNF-α (MP6-XT22), fluorescein isothiocyanate (FITC) CD4 (RM4-5), APC IL-4 (11B11), FITC CD8a (53-6.7), phycoerythrin (PE) IFN-γ (XMG1.2), FITC CD11c (N418), PE CD11c (N418), PE TNF-α (MP6-XT22), APC IL-6 (MP5-20F3), FITC CD86 (PO3), APC CD40 (3/23), PE CD8 (53-6.7), APC B220 (RA3-6B2), TNF-α–neutralizing antibody (TN3-19.12), and IL-6–neutralizing antibody (MP5-20F3); human—FITC CD86 (BU63) and PE CD40 (HB14).

BMDC cell surface marker and cytokine staining

Monocytes were harvested from 6-week-old C57BL/6 mice. Monocytes were differentiated into dendritic cells (BMDCs) using supplemented culture medium: RPMI 1640 (Life Technologies), 10% HIFBS (Sigma-Aldrich), GM-CSF (20 ng/ml; produced using "66" cell line), 2 mM L-glutamine (Life Technologies), 1% antibiotic-antimycotic (Life Technologies), and 50 μM β-mercaptoethanol (Sigma-Aldrich). After 5 days of culture, BMDCs were incubated with SN50 (250 μg/ml). After 1 hour, CpG ODN 1826 (Integrated DNA Technologies, IDT) and GolgiPlug (1 μl/ml; BD Biosciences) were added. Cells were incubated for 6 hours at 37°C and 5% CO_2. Cells were stained for CD40, CD86, and intracellular IL-6 and TNF-α cytokine production and analyzed using BD Accuri C6 flow cytometer.

NHP cell surface marker and cytokine analysis

Blood samples were collected in EDTA-coated collection tubes from rhesus macaques. Whole blood was diluted to a final ratio of 1 part blood to 1 part PBS and layered over Lympholyte-Mammal Cell Separation Media (Cedarlane). Samples were centrifuged at 800*g* for 20 min at room temperature (RT), and the buffy coat was collected and washed. Cells were counted and cryopreserved in 45% RPMI 1640 media, 45% fetal bovine serum, and 10% dimethyl sulfoxide and stored in liquid nitrogen until tested. Samples were treated with SN50 (125 μg/ml) and incubated at 37°C and 5% CO_2 for 1 hour. After 1 hour, LPS (1 μg/ml) was added, and cells were incubated for 12 hours. Supernatant was tested for cytokine secretion using BD Nonhuman Primate Th1/Th2 Cytokine Kit. Cells were pelleted and stained for CD86 expression using BD Cytofix/Cytoperm Fixation/Permeabilization Solution Kit according to the manufacturer's protocol.

THP-1 cytokine and cell surface marker analysis

THP-1 cells (2×10^6 cells) were plated in a 12-well plate in 500 μl of RPMI containing 10% HIFBS. SN50 (100 μg/ml) was added and incubated at 37°C and 5% CO_2 for 1 hour. After 1 hour, LPS was added to wells (1 μg/ml). After 6 hours, cell supernatant was removed and analyzed for cytokines using Human Inflammatory Cytometric Bead Array (BD Bioscience). Cells were stained for CD86 and CD40 using BD Cytofix/Cytoperm Fixation/Permeabilization Solution Kit according to the manufacturer's protocol.

Scanning electron microscopy analysis

Sample suspensions obtained directly from injection mixtures were dried for 24 hours, mounted on carbon tape, and sputter coated (South Bay Technologies) with approximately 2 to 4 nm of Au/Pd 60:40 or Ir. Scanning electron microscopy of the sample suspensions was performed using an FEI Quanta 3D FEG dual beam (scanning electron microscope/focused ion beam) equipped with Inca EDS (Oxford Instruments).

In vivo studies

Animals

All animal procedures were performed under a protocol approved by the University of Chicago Institutional Animal Care and Use Committee (IACUC). Six- to 8-week-old C57/B6 female mice were purchased from the Jackson laboratory. All compounds were tested for endotoxin before use. All vaccinations were administered intramuscularly in the hind leg. Blood was collected from the saphenous vein at time points indicated.

Antigens were purchased from Sino Biological {HIV subgroup M, influenza A H1N1 (A/California/04/2009) hemagglutinin (HA) protein, dengue virus DENV-2 (strain New Guinea C) capsid protein/DENV-C protein (His tag), Virogen [HIV-1 env (gp41) antigen]} or Invitrogen (VacciGrade Ovalbumin). VacciGrade CpG ODN 1826 was purchased from InvivoGen or AdipoGen. SN50 was synthesized via solid-phase peptide synthesis as previously described (*69*) and purified using Gilson preparatory high-performance liquid chromatography (HPLC).

Vaccinations

Mice were lightly anesthetized with isoflurane and injected intramuscularly in the hind leg with 50 μl containing antigen, adjuvant, and PBS. Antigen doses were as follows: OVA (100 μg), DENV-2 C (5 μg), and gp120 (3 μg). CpG dose was 50 μg; SN50, 500 μg (unless otherwise stated); TNF-αN, 30 μg; and IL-6 N, 30 μg.

Plasma cytokine analysis

Blood was collected from mice at specified time points in 0.2 ml of heparin-coated collection tubes (VWR Scientific). Serum was isolated via centrifugation 2000*g* for 5 min. Supernatant was collected and stored at −80°C until use. Serum was analyzed using BD Cytometric Bead Array Mouse Th1/Th2/Th17 Cytokine Kit or Mouse Inflammation Cytokine Kit according to the manufacturer's protocol. Briefly, beads containing antibodies for desired cytokines were mixed with 50 μl of serum and 50 μl of PE detection reagent and incubated for 2 hours. Beads were washed and analyzed using BD Accuri C6 flow cytometer. Data were analyzed using BD Accuri C6 software and GraphPad Prism.

Antibody quantification

Mice were vaccinated with indicated formulations. Blood was collected at time points indicated in 0.2 ml of heparin-coated collection tubes (VWR Scientific) for plasma or uncoated tubes for serum. Plasma was isolated via centrifugation (2000*g*, 5 min). Serum was isolated by allowing blood to clot for 15 to 30 min at RT and centrifuging (2000*g* for 10 min) at 4°C. Serum was analyzed using a quantitative anti-OVA total Ig's ELISA kit (Alpha Diagnostic International) according to the specified protocol. Total IgG and IgA were analyzed using total mouse IgG or IgA uncoated ELISA (Invitrogen) and was analyzed using a Multiskan FC plate reader (Thermo Fisher

Scientific), and absorbance was measured at 450 nm. Data were analyzed using GraphPad Prism.

Lymph node gene expression

Mice were vaccinated as described above, and the draining inguinal lymph node was harvested 24 hours after vaccination and placed in PBS on ice. A single-cell suspension was created by pushing the lymph node through a 70-μm filter in a six-well plate, and filter was washed with 500 μl of PBS. Cells were pelleted and resuspended in TRIzol, and RNA was isolated using a Zymo Direct-zol RNA Microprep kit. SuperScript IV First-Strand Synthesis System was used for synthesis of first-strand cDNA. A Mouse Immune TaqMan Array (Thermo Fisher Scientific) and a Lifetech Viia7 (Applied Biosystems) thermocyler were used to analyze gene expression according to the manufacturer's protocol. Data were analyzed using *Agilent Introduction to Quantitative PCR Methods and Applications Guide* using ddCt method as outlined at www.agilent.com/genomics.

Antigen recall assay

Mice were vaccinated and boosted on day 14 as described above. On day 21, spleens were harvested and placed in PBS on ice. Spleens were crushed between two frosted glass slides and pushed through a 70-μm filter. Cells were pelleted at 400*g* for 10 min and resuspended in prewarmed BD Pharm Lyse lysing solution and incubated at 37°C for 3 min. PBS (30 ml) was added, and cells were pelleted at 400*g* for 10 min. Cells were resuspended at 2×10^6 cells/ml in RPMI supplemented with 10% HIFBS. Cells were added to a flat-bottom 96-well plate precoated with anti-CD3 (3 μg/ml). Antigen or epitope (20 μg/ml) and anti-CD28 (5 μg/ml) were added, and cells were incubated for 48 hours. After 48 hours, cells were pelleted at 400*g* for 10 min, and cell supernatant was removed and analyzed using LEGENDplex Mouse Th Cytokine Panel according to the manufacturer's protocol.

Epitope analysis

Mouse serum was collected as described above, and samples were analyzed using Multiwell RepliTope microarray for appropriate antigen (JPT Innovative Peptide Solutions) according to the manufacturer's protocol. Briefly, serum samples were diluted in 3% BSA in 1× tris-buffered saline (TBS) buffer + 0.1% Tween 20 (TBS-T) to a final concentration of 10 μg/ml. The microarray was fitted with an ArraySlide 24-4 chamber (JPT Innovative Peptide Solutions) to enable multisample analysis. Diluted serum (50 μl) was added to sample wells and incubated for 1 hour at 30°C. Wells were washed five times with TBS-T. Secondary antibody (150 μl, 1 μg/ml) was added to wells and incubated at RT for 1 hour. Wells were washed five times with TBS-T and two times with Nanopure water. Arrays were imaged using a Caliber I.D. RS-G4 confocal microscope and analyzed using ImageJ.

Influenza challenge model

Animals

All animal procedures were performed under a protocol approved by the Illinois Institute of Technology Research IACUC. Six- to 8-week-old C57/B6 female mice were purchased from Charles River. All compounds were tested for endotoxin before use. All vaccinations were administered intramuscularly in the hind leg.

Initial group assignments were assigned to using a computerized randomization procedure based on body weights that produce similar group mean values [ToxData version 3.0 (PDS Pathology Data Systems Inc., Basel, Switzerland)]. Mice were vaccinated by intramuscular injection into the hind leg on days 0 and 21. The vaccine material used in this study is Fluzone Quadrivalent influenza vaccine (Sanofi Pasteur). Each 0.5-ml dose of Fluzone contains at least 15 μg of HA from each of the following four influenza strains recommended for the 2017/2018 influenza season: A/Michigan/45/2015 X-275 (H1N1)pdm09-like strain, A/Hong Kong/4801/2014 X-263B (H3N2)-like strain, B/Phuket/3073/2013-like strain, and B/Brisbane/60/2008-like strain. At least 1 μg of each strain was used in vaccination of the mice.

Body weights were collected 24, 48, and 72 hours after prime vaccination. Body temperatures were collected 1, 3, 24, 48, and 72 hours after prime vaccination. Blood samples were collected on days 0, 14, 28, 42, and 56. Plasma was collected on day 0. Serum was collected on days 14, 28, 52, and 56. Five animals from each group were humanely euthanized on day 14 after vaccination. Spleens were collected for T cell analysis. On day 43 after vaccination, all mice were challenged via intranasal route with a lethal dose of A/Michigan/45/2015. The dose level of challenge virus used was an equivalent of 5 LD_{50}. For inoculation, mice were anesthetized with a ketamine (80 mg/kg) and xylazine (10 mg/kg) mixture. Once anesthetized, 0.025 ml of inoculum was delivered dropwise into the nares. The mouse was held upright to allow the virus to be inhaled thoroughly and then returned to its cage. After challenge, body weights and temperature readings were recorded daily through a transponder (Bio Medic Data Systems, Seaford, DE) implanted subcutaneously in each mouse. Animals were monitored for morbidity/mortality for 14 days after infection. Any animals meeting predetermined moribund criteria (>20% weight loss) were humanely euthanized. Three animals from each group were humanely euthanized on day 3 after challenge (day 45), and lungs were collected for viral quantitation by plaque assay/median tissue culture infectious dose ($TCID_{50}$). Tissues for viral titers were weighed then flash frozen in an ethanol/dry ice bath or liquid nitrogen and stored at ≤−65°C. Frozen organs were thawed at 37°C for 5 min. Once thawed, organs were homogenized in minimum essential medium 10% (w/v) using a Bead Ruptor 12 (Omni International, Kennesaw, Georgia) in tubes containing 1.4-mm ceramic beads. Homogenized organs were centrifuged at 2000*g* for 5 min to remove cellular debris. The resulting supernatant was serially diluted 10-fold and then transferred into respective wells of a 96-well plate containing a monolayer of Madin-Darby canine kidney cells (MDCK) cells for titration. The $TCID_{50}$ assay will be performed. $TCID_{50}$ titers will be calculated using the method of Reed-Meunch. The remaining five mice in each group were monitored for the remaining days of the challenge.

Neutralization assays

Serum samples were tested against a representative of each dengue serotype (DENV-1: strain Hawaii, DENV-2 strain New Guinea C, DENV-3 strain Philippines/H87/1956, and DENV-4 strain H241). Sera were serially diluted twofold (starting dilution 1:100) and then incubated with standardized virus concentration of 50 to 120 PFU of each strain. The serum:virus mixture was transferred into respective wells of a 96-well plate that contained a monolayer of Vero cells. The cells were incubated for 40 hours at 37°C. After 40 hours of incubation, the cells were fixed with 1.0% paraformaldehyde and stained by Anti-Flavivirus Group Antigen Antibody, clone D1-4G2-4-15 (Millipore Billerica, MA) followed by peroxidase-conjugated goat anti-mouse IgG (Kirkegaard and Perry Laboratories, Gaithersburg, MD). Spots were developed using TrueBlue Peroxidase Substrate (Kirkegaard and Perry Laboratories, Gaithersburg, MD). Plaques were visualized and counted using an ELISPOT instrument. Plaque

reduction neutralization test (PRNT) titers were expressed in terms of conventional 50% PRNT end point titers.

Tolerability and protection score

We assigned a tolerability score composed of systemic TNF-α, IL-6 levels, and weight loss after vaccination. A score for each TNF-α, IL-6, and weight loss was assigned for each mouse. The tolerability score of a single mouse represents the summation of these individual scores. A protection score was assigned on the basis of survival, change in body weight, and change in body temperature after challenge. Scores were determined by dividing values into quartiles and assigning a number from 0 to 4 based on the quartile. Higher values indicate an improved safety profile (lower TNF-α or IL-6 and less weight loss after vaccination) or improved protection (survival, less weight loss, and higher body temperature after challenge).

Statistics and replicates

Data are plotted and reported in the text as the means ± SEM. Sample size is as indicated in biological replicates in all in vivo and in vitro experiments. The sample sizes were chosen on the basis of preliminary experiments or literature precedent indicating that the number would be sufficient to detect significant differences in mean values should they exist. *P* values were calculated using a one-way analysis of variance (ANOVA) and Tukey post hoc test or two-tailed unpaired heteroscedastic *t* test where appropriate. All experiments have been repeated (sometimes with minor variations because of reagents and materials), and replication was successful.

SUPPLEMENTARY MATERIALS

Supplementary material for this article is available at http://advances.sciencemag.org/cgi/content/full/6/37/eaaz8700/DC1

View/request a protocol for this paper from *Bio-protocol*.

REFERENCES AND NOTES

1. R. Edelman, Vaccine adjuvants. *Rev. Infect. Dis.* **2**, 370–383 (1980).
2. A. M. Harandi, G. Davies, O. F. Olesen, Vaccine adjuvants: Scientific challenges and strategic initiatives. *Expert Rev. Vaccines* **8.3**, 293–298 (2009).
3. D. T. O'Hagan, E. De Gregorio, The path to a successful vaccine adjuvant – "The long and winding road". *Drug Discov. Today* **14**, 541–551 (2009).
4. N. Petrovsky, J. C. Aguilar, Vaccine adjuvants: Current state and future trends. *Immunol. Cell Biol.* **82**, 488–496 (2004).
5. R. L. Coffman, A. Sher, R. A. Seder, Vaccine adjuvants: Putting innate immunity to work. *Immunity* **33**, 492–503 (2010).
6. A. Pashine, N. M. Valiante, J. B. Ulmer, Targeting the innate immune response with improved vaccine adjuvants. *Nat. Med.* **11**, S63–S68 (2005).
7. K. Hoebe, E. Janssen, B. Beutler, The interface between innate and adaptive immunity. *Nat. Immunol.* **5**, 971–974 (2004).
8. P. M. D'Agostino, C. Kwak, H. A. Vecchiarelli, J. G. Toth, J. M. Miller, Z. Masheeb, B. S. McEwen, K. Bulloch, Viral-induced encephalitis initiates distinct and functional $CD103^+$ $CD11b^+$ brain dendritic cell populations within the olfactory bulb. *Proc. Natl. Acad. Sci. U.S.A.* **109**, 6175–6180 (2012).
9. J. Banchereau, R. M. Steinman, Dendritic cells and the control of immunity. *Nature* **392**, 245–252 (1998).
10. G. Del Giudice, R. Rappuoli, A. M. Didierlaurent, Correlates of adjuvanticity: A review on adjuvants in licensed vaccines. *Semin. Immunol.* **39**, 14–21 (2018).
11. D. van Duin, R. Medzhitov, A. C. Shaw, Triggering TLR signaling in vaccination. *Trends Immunol.* **27**, 49–55 (2006).
12. C. J. Dale, R. De Rose, K. M. Wilson, H. A. Croom, S. Thomson, B. E. H. Coupar, A. Ramsay, D. F. J. Purcell, R. Ffrench, M. Law, S. Emery, D. A. Cooper, I. A. Ramshaw, D. B. Boyle, S. J. Kent; For the Australian Thai HIV Vaccine Consortium, Evaluation in macaques of HIV-1 DNA vaccines containing primate CpG motifs and fowlpoxvirus vaccines co-expressing IFNγ or IL-12. *Vaccine* **23**, 188–197 (2004).
13. C. Bode, G. Zhao, F. Steinhagen, T. Kinjo, D. M. Klinman, CpG DNA as a vaccine adjuvant. *Expert Rev. Vaccines* **10**, 499–511 (2011).
14. R. Weeratna, L. Comanita, H. L. Davis, CPG ODN allows lower dose of antigen against hepatitis B surface antigen in BALB/c mice. *Immunol. Cell Biol.* **81**, 59–62 (2003).
15. D. M. Klinman, H. Xie, B. E. Ivins, CpG oligonucleotides improve the protective immune response induced by the licensed anthrax vaccine. *Ann. N. Y. Acad. Sci.* **1082**, 137–150 (2006).
16. E. Davila, R. Kennedy, E. Celis, Generation of antitumor immunity by cytotoxic T lymphocyte epitope peptide vaccination, CpG-oligodeoxynucleotide adjuvant, and CTLA-4 blockade. *Cancer Res.* **63**, 3281–3288 (2003).
17. A. M. Krieg, Toll-like receptor 9 (TLR9) agonists in the treatment of cancer. *Oncogene* **27**, 161–167 (2008).
18. R. D. Ellis, Y. Wu, L. B. Martin, D. Shaffer, K. Miura, J. Aebig, A. Orcutt, K. Rausch, D. Zhu, A. Mogensen, M. P. Fay, D. L. Narum, C. Long, L. Miller, A. P. Durbin, Phase 1 study in malaria naïve adults of BSAM2/Alhydrogel®+CPG 7909, a blood stage vaccine against *P. falciparum* malaria. *PLOS ONE* **7**, e46094 (2012).
19. A. S. Cross, N. Greenberg, M. Billington, L. Zhang, C. De Filippi, R. C. May, K. K. Bajwa, Phase 1 testing of detoxified LPS/group B meningococcal outer membrane protein vaccine with and without synthetic CPG 7909 adjuvant for the prevention and treatment of sepsis. *Vaccine* **33**, 6719–6726 (2015).
20. M. L. Mbow, E. De Gregorio, N. M. Valiante, R. Rappuoli, New adjuvants for human vaccines. *Curr. Opin. Immunol.* **22**, 411–416 (2010).
21. H. Kanzler, F. J. Barrat, E. M. Hessel, R. L. Coffman, Therapeutic targeting of innate immunity with Toll-like receptor agonists and antagonists. *Nat. Med.* **13**, 552–559 (2007).
22. L. M. Christian, K. Porter, E. Karlsson, S. Schultz-Cherry, Proinflammatory cytokine responses correspond with subjective side effects after influenza virus vaccination. *Vaccine* **33**, 3360–3366 (2015).
23. W. L. Simon, H. M. Salk, I. G. Ovsyannikova, R. B. Kennedy, G. A. Poland, Cytokine production associated with smallpox vaccine responses. *Immunotherapy* **6**, 1097–1112 (2014).
24. A. D. Pasquale, S. Preiss, F. T. Da Silva, N. Garçon, Vaccine Adjuvants: From 1920 to 2015 and Beyond. *Vaccine* **3**, 320–343 (2015).
25. G. M. Barton, R. Medzhitov, Toll-like receptor signaling pathways. *Science* **300**, 1524–1525 (2003).
26. T. Lawrence, The nuclear factor NF-κB pathway in inflammation. *Cold Spring Harb. Perspect. Biol.* **1**, a001651 (2009).
27. S. Akira, K. Takeda, Toll-like receptor signalling. *Nat. Rev. Immunol.* **4**, 499–511 (2004).
28. A. Hoffmann, T. H. Leung, D. Baltimore, Genetic analysis of NF-κB/Rel transcription factors defines functional specificities. *EMBO J.* **22**, 5530–5539 (2003).
29. A. Hoffmann, D. Baltimore, Circuitry of nuclear factor κB signaling. *Immunol. Rev.* **210**, 171–186 (2006).
30. P. A. Baeuerle, T. Henkel, Function and activation of NF-κB in the immune system. *Annu. Rev. Immunol.* **12**, 141–179 (1994).
31. X. Dolcet, D. Llobet, J. Pallares, X. Matias-Guiu, NF-κB in development and progression of human cancer. *Virchows Arch.* **446**, 475–482 (2005).
32. C.-Y. Wang, M. W. Mayo, A. S. Baldwin Jr., TNF- and cancer therapy–induced apoptosis: Potentiation by inhibition of NF-κB. *Science* **274**, 784–787 (1996).
33. Y. Xia, S. Shen, I. M. Verma, NF-κB, an active player in human cancers. *Cancer Immunol. Res.* **2**, 823–830 (2014).
34. D. J. Erstad, J. C. Cusack Jr., Targeting the NF-κB pathway in cancer therapy. *Surg. Oncol. Clin. N. Am.* **22**, 705–746 (2013).
35. S. Bacher, M. L. Schmitz, The NF-κB pathway as a potential target for autoimmune disease therapy. *Curr. Pharm. Des.* **10**, 2827–2837 (2004).
36. T. Letoha, E. Kusz, G. Pápai, A. Szabolcs, J. Kaszaki, I. Varga, T. Takács, B. Penke, E. Duda, In vitro and in vivo nuclear factor-κB inhibitory effects of the cell-penetrating penetratin peptide. *Mol. Pharmacol.* **69**, 2027–2036 (2006).
37. S. F. Liu, X. Ye, A. B. Malik, In vivo inhibition of nuclear factor-κ B activation prevents inducible nitric oxide synthase expression and systemic hypotension in a rat model of septic shock. *J. Immunol.* **159**, 3976–3983 (1997).
38. A. Eigler, B. Sinha, G. Hartmann, S. Endres, Taming TNF: Strategies to restrain this proinflammatory cytokine. *Immunol. Today* **18**, 487–492 (1997).
39. P. P. Tak, G. S. Firestein, NF-κB: A key role in inflammatory diseases. *J. Clin. Invest.* **107**, 7–11 (2001).
40. J. Wang, X. Wang, S. Hussain, Y. Zheng, S. Sanjabi, F. Ouaaz, A. A. Beg, Distinct roles of different NF-κB subunits in regulating inflammatory and T cell stimulatory gene expression in dendritic cells. *J. Immunol.* **178**, 6777–6788 (2007).
41. J. Zienkiewicz, A. Armitage, J. Hawiger, Targeting nuclear import shuttles, importins/karyopherins alpha by a peptide mimicking the NF κB1/p50 nuclear localization sequence. *J. Am. Heart Assoc.* **2**, e000386 (2013).
42. Y. Z. Lin, S. Y. Yao, R. A. Veach, T. R. Torgerson, J. Hawiger, Inhibition of nuclear translocation of transcription factor NF-κB by a synthetic peptide containing a cell membrane-permeable motif and nuclear localization sequence. *J. Biol. Chem.* **270**, 14255–14258 (1995).
43. T. R. Torgerson, A. D. Colosia, J. P. Donahue, Y. Z. Lin, J. Hawiger, Regulation of NF-κ B, AP-1, NFAT, and STAT1 nuclear import in T lymphocytes by noninvasive delivery

of peptide carrying the nuclear localization sequence of NF-κ B p50. *J. Immunol.* **161**, 6084–6092 (1998).
44. V. Kolenko, T. Bloom, P. Rayman, R. Bukowski, E. Hsi, J. Finke, Inhibition of NF-κB activity in human T lymphocytes induces caspase-dependent apoptosis without detectable activation of caspase-1 and -3. *J. Immunol.* **163**, 590–598 (1999).
45. A. Oeckinghaus, S. Ghosh, The NF-κB family of transcription factors and its regulation. *Cold Spring Harb. Perspect. Biol.* **1**, a000034 (2009).
46. R. Brignall, A. T. Moody, S. Mathew, S. Gaudet, Considering abundance, affinity, and binding site availability in the NF-κB target selection puzzle. *Front. Immunol.* **10**, 609 (2019).
47. H. L. Pahl, Activators and target genes of Rel/NF-κB transcription factors. *Oncogene* **18**, 6853–6866 (1999).
48. J.-I. Satoh, Molecular network of ChIP-Seq-based NF-κB p65 target genes involves diverse immune functions relevant to the immunopathogenesis of multiple sclerosis. *Mult. Scler. Relat. Disord.* **3**, 94–106 (2014).
49. G. Gu, T. Wang, Y. Yang, X. Xu, J. Wang, An Improved SELEX-Seq strategy for characterizing DNA-binding specificity of transcription factor: NF-κB as an example. *PLOS ONE* **8**, e76109 (2013).
50. D. Wong, A. Teixeira, S. Oikonomopoulos, P. Humburg, I. N. Lone, D. Saliba, T. Siggers, M. Bulyk, D. Angelov, S. Dimitrov, I. A. Udalova, J. Ragoussis, Extensive characterization of NF-κB binding uncovers non-canonical motifs and advances the interpretation of genetic functional traits. *Genome Biol.* **12**, R70 (2011).
51. W. Du, J. Gao, T. Wang, J. Wang, Single-nucleotide mutation matrix: A new model for predicting the NF-κB DNA binding sites. *PLOS ONE* **9**, e101490 (2014).
52. M. C. Mulero, V. Y.-F. Wang, T. Huxford, G. Ghosh, Genome reading by the NF-κB transcription factors. *Nucleic Acids Res.* **47**, 9967–9989 (2019).
53. D. Bhatt, S. Ghosh, Regulation of the NF-κB-mediated transcription of inflammatory genes. *Front. Immunol.* **5**, 71 (2014).
54. M. Pasparakis, T. Luedde, M. Schmidt-Supprian, Dissection of the NF-κB signalling cascade in transgenic and knockout mice. *Cell Death Differ.* **13**, 861–872 (2006).
55. A. Nijnik, R. Mott, D. P. Kwiatkowski, I. A. Udalova, Comparing the fine specificity of DNA binding by NF-κB p50 and p52 using principal coordinates analysis. *Nucleic Acids Res.* **31**, 1497–1501 (2003).
56. P. Tripathi, A. Aggarwal, NF-kB transcription factor: A key player in the generation of immune response. *Curr. Sci.* **90**, 519–531 (2006).
57. J. Hiscott, H. Kwon, P. Génin, Hostile takeovers: Viral appropriation of the NF-κB pathway. *J. Clin. Invest.* **107**, 143–151 (2001).
58. M. G. Netea, B. J. Kullberg, J. W. Van der Meer, Circulating cytokines as mediators of fever. *Clin. Infect. Dis.* **31**, S178–S184 (2000).
59. H. Jung, D. Kim, Y. Y. Kang, H. Kim, J. B. Lee, H. Mok, CpG incorporated DNA microparticles for elevated immune stimulation for antigen presenting cells. *RSC Adv.* **8**, 6608–6615 (2018).
60. D. A. Kahn, D. C. Archer, D. P. Gold, C. J. Kelly, Adjuvant immunotherapy is dependent on inducible nitric oxide synthase. *J. Exp. Med.* **193**, 1261–1268 (2001).
61. T. Sparwasser, L. Hültner, E. S. Koch, A. Luz, G. B. Lipford, H. Wagner, Immunostimulatory CpG-oligodeoxynucleotides cause extramedullary murine hemopoiesis. *J. Immunol.* **162**, 2368–2374 (1999).
62. N. M. Bouvier, A. C. Lowen, Animal models for influenza virus pathogenesis and transmission. *Viruses* **2**, 1530–1563 (2010).
63. G. Daniele, R. G. Mendoza, D. Winnier, T. V. Fiorentino, Z. Pengou, J. Cornell, F. Andreozzi, C. Jenkinson, E. Cersosimo, M. Federici, D. Tripathy, F. Folli, The inflammatory status score including IL-6, TNF-α, osteopontin, fractalkine, MCP-1 and adiponectin underlies whole-body insulin resistance and hyperglycemia in type 2 diabetes mellitus. *Acta Diabetol.* **51**, 123–131 (2014).
64. G. Segev, P. H. Kass, T. Francey, L. D. Cowgill, A novel clinical scoring system for outcome prediction in dogs with acute kidney injury managed by hemodialysis. *J. Vet. Intern. Med.* **22**, 301–308 (2008).
65. K. M. Page, L. Zhang, A. Mendizabal, S. Wease, S. Carter, K. Shoulars, T. Gentry, A. E. Balber, J. Kurtzberg, The cord blood Apgar: A novel scoring system to optimize selection of banked cord blood grafts for transplantation (CME). *Transfusion* **52**, 272–283 (2012).
66. A. Ramachandran, C. Snehalatha, A. D. S. Baskar, S. Mary, C. K. S. Kumar, S. Selvam, S. Catherine, V. Vijay, Temporal changes in prevalence of diabetes and impaired glucose tolerance associated with lifestyle transition occurring in the rural population in India. *Diabetologia* **47**, 860–865 (2004).
67. T. D. Gilmore, M. Herscovitch, Inhibitors of NF-κB signaling: 785 and counting. *Oncogene* **25**, 6887–6899 (2006).
68. S. Gnjatic, N. B. Sawhney, N. Bhardwaj, Toll-like receptor agonists: Are they good adjuvants? *Cancer J.* **16**, 382–391 (2010).
69. X. Y. Liu, D. Robinson, R. A. Veach, D. Liu, S. Timmons, R. D. Collins, J. Hawiger, Peptide-directed suppression of a pro-inflammatory cytokine response. *J. Biol. Chem.* **275**, 16774–16778 (2000).
70. A. Gorlani, D. N. Forthal, Antibody-dependent enhancement and the risk of HIV infection. *Curr. HIV Res.* **11**, 421–426 (2013).
71. L. L. Lu, T. J. Suscovich, S. M. Fortune, G. Alter, Beyond binding: Antibody effector functions in infectious diseases. *Nat. Rev. Immunol.* **18**, 46–61 (2018).
72. D. S. Burke, Human HIV vaccine trials: Does antibody-dependent enhancement pose a genuine risk? *Perspect. Biol. Med.* **35**, 511–530 (1992).
73. M. Trovato, L. D'Apice, A. Prisco, P. De Berardinis, HIV vaccination: A roadmap among advancements and concerns. *Int. J. Mol. Sci.* **19**, 1241 (2018).
74. V. Holl, M. Peressin, T. Decoville, S. Schmidt, S. Zolla-Pazner, A.-M. Aubertin, C. Moog, Nonneutralizing antibodies are able to inhibit human immunodeficiency virus type 1 replication in macrophages and immature dendritic cells. *J. Virol.* **80**, 6177–6181 (2006).
75. L. M. Mayr, B. Su, C. Moog, Non-neutralizing antibodies directed against HIV and their functions. *Front. Immunol.* **8**, (2017).
76. D. R. Burton, L. Hangartner, Broadly neutralizing antibodies to HIV and their role in vaccine design. *Annu. Rev. Immunol.* **34**, 635–659 (2016).
77. H. M. Cheeseman, N. J. Olejniczak, P. M. Rogers, A. B. Evans, D. F. L. King, P. Ziprin, H.-X. Liao, B. F. Haynes, R. J. Shattock, Broadly neutralizing antibodies display potential for prevention of HIV-1 infection of mucosal tissue superior to that of nonneutralizing antibodies. *J. Virol.* **91**, e01762–e01716 (2016).
78. D. Sok, D. R. Burton, HIV broadly neutralizing antibodies: Taking good care of the 98%. *Immunity* **45**, 958–960 (2016).
79. J. Huang, B. H. Kang, M. Pancera, J. H. Lee, T. Tong, Y. Feng, H. Imamichi, I. S. Georgiev, G.-Y. Chuang, A. Druz, N. A. Doria-Rose, L. Laub, K. Sliepen, M. J. van Gils, A. T. de la Peña, R. Derking, P.-J. Klasse, S. A. Migueles, R. T. Bailer, M. Alam, P. Pugach, B. F. Haynes, R. T. Wyatt, R. W. Sanders, J. M. Binley, A. B. Ward, J. R. Mascola, P. D. Kwong, M. Connors, Broad and potent HIV-1 neutralization by a human antibody that binds the gp41-gp120 interface. *Nature* **515**, 138–142 (2014).
80. Y. Li, S. O'Dell, L. M. Walker, X. Wu, J. Guenaga, Y. Feng, S. D. Schmidt, K. M. Kee, M. K. Louder, J. E. Ledgerwood, B. S. Graham, B. F. Haynes, D. R. Burton, R. T. Wyatt, J. R. Mascola, Mechanism of neutralization by the broadly neutralizing HIV-1 monoclonal antibody VRC01. *J. Virol.* **85**, 8954–8967 (2011).
81. X. Wu, Z.-Y. Yang, Y. Li, C.-M. Hogerkorp, W. R. Schief, M. S. Seaman, T. Zhou, S. D. Schmidt, L. Wu, L. Xu, N. S. Longo, K. M. Kee, S. O'Dell, M. K. Louder, D. L. Wycuff, Y. Feng, M. Nason, N. Doria-Rose, M. Connors, P. D. Kwong, M. Roederer, R. T. Wyatt, G. J. Nabel, J. R. Mascola, Rational design of envelope identifies broadly neutralizing human monoclonal antibodies to HIV-1. *Science* **329**, 856–861 (2010).
82. S. E. Ryu, W. A. Hendrickson, Structure and design of broadly-neutralizing antibodies against HIV. *Mol. Cells* **34**, 231–237 (2012).

Acknowledgments: We thank A. Burkhardt and A. Gilkes for training and assistance with in vivo techniques. We thank R. Nakajima for assistance with imaging microarrays and D. Piraner for help with image analysis. We thank A. Chon for assistance with HPLC optimization and N. Nihesh for training and assistance with peptide synthesis. We acknowledge J. Qin at the University of Chicago for training and assistance with mass spectrometry. **Funding:** We would like to acknowledge support by the NIH (1U01AI124286-01 and 1DP2AI112194-01, GM099594). This work was supported by the Defense Threat Reduction Agency (DTRA) under contract supporting this work (HDTRA11810052). A.P.E.-K. thanks the Pew Scholars Program and the Cottrell Scholars Program for support. B.A.M. thanks NSF-GRFP (DGE-1321846), and B.J.C. thanks NSF-GRFP (DGE-1746045). We would like to thank NSF instrumentation grant CHE-1048528. This work was supported, in part, by a grant from the Alfred P. Sloan Foundation. **Author contributions:** B.A.M. and A.P.E.-K. conceived of and designed the project and experiments and wrote the manuscript. B.A.M., R.C.S., Y.E.-B., D.A.B., K.M.B., and B.G.M. performed the experiments. B.A.M., B.J.C., M.G.R., and S.Y. synthesized materials. **Competing interests:** B.A.M. and A.E.K. are inventors on a pending patent related to this work filed by the University of Chicago (no. PCT/US19/64888, filed 16 December 2019). The authors declare that they have no other competing interests. **Data and materials availability:** All data needed to evaluate the conclusions in the paper are present in the paper and/or the Supplementary Materials. Additional data related to this paper may be requested from the authors.

Submitted 17 October 2019
Accepted 24 July 2020
Published 9 September 2020
10.1126/sciadv.aaz8700

Citation: B. A. Moser, R. C. Steinhardt, Y. Escalante-Buendia, D. A. Boltz, K. M. Barker, B. J. Cassaidy, M. Rosenberger, S. Yoo, B. G. McGonnigal, A. P. Esser-Kahn, Increased vaccine tolerability and protection via NF-κB modulation. *Sci. Adv.* **6**, eaaz8700 (2020).

Science Advances

Increased vaccine tolerability and protection via NF-κB modulation

B. A. Moser, R. C. Steinhardt, Y. Escalante-Buendia, D. A. Boltz, K. M. Barker, B. J. Cassaidy, M.G. Rosenberger, S. Yoo, B. G. McGonnigal and A. P. Esser-Kahn

Sci Adv **6** (37), eaaz8700.
DOI: 10.1126/sciadv.aaz8700

Science Advances (ISSN 2375-2548) is published by the American Association for the Advancement of Science, 1200 New York Avenue NW, Washington, DC 20005. The title *Science Advances* is a registered trademark of AAAS.